THE JOURNAL OF PHYSICAL CHEMISTRY C

Article

Cite This: J. Phys. Chem. C XXXX, XXX, XXX−XXX

pubs.acs.org/JPCC

Can Hydrogen Catalyze Transitions between h-BN and c-BN in Volume Plasma?

Predrag Krstic*[,†] and Longtao Han[†,‡]

[†]Institute for Advanced Computational Science, Stony Brook University, Stony Brook, New York 11794-5250, United States

[‡]Department of Materials Science and Chemical Engineering, Stony Brook University, Stony Brook, New York 11794-2275, United States

Supporting Information

ABSTRACT: In a range of temperatures from 1500 to 2500 K, processes of transformation between various nanometer-scale boron nitride structures in the presence of hydrogen are simulated. We find that hydrogen catalyzes the transition from the sp^2 hybridization of B and N atoms in hexagonal boron nitride (h-BN) to sp^3 hybridization, creating tetrahedral amorphous boron nitride (ta-BN) or cubic boron nitride (c-BN), at 1500 and 2000 K, respectively. At 2000 K in the presence of hydrogen, ta-BN can evolve to c-BN, usually partially encapsulated by a h-BN cage. All of these transformational processes of boron nitrides have analogs in graphene-diamond conversions. Change of atom hybridization can also proceed in the opposite direction under different conditions. Using quantum-classical molecular dynamics based on the density functional tight-binding method, we analyze the evolution of the nanoscale particles via the hybridization state of B/N atoms, ring composition, exchange of particles with environment, as well as the energetics of the processes. The simulations allow the estimation of temperature windows favorable for stable h-BN, c-BN, and amorphous BN when interacting with hydrogen.

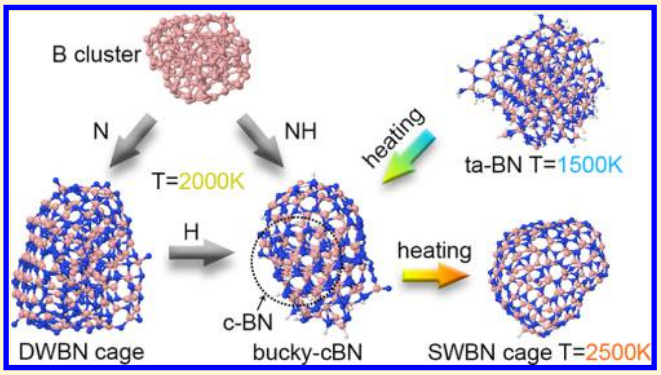

INTRODUCTION

Boron and nitrogen are immediate neighbors of carbon in the periodic table, with three and five valence electrons, respectively. Therefore, BN is isoelectronic with bonded carbon atoms. As a consequence, BN and C materials have analogous crystal modifications. 2D h-BN corresponds to graphene and is characterized by a network of B_3N_3 hexagonal rings formed by sp^2-hybridized B and N atoms. Each boron atom is bonded to three neighboring nitrogen atoms and vice versa. The h-BN is similar to graphite,[1] while cubic boron nitride (c-BN) is a cubic lattice analogous to diamond and is formed by sp^3-hybridized B and N atoms. Each atom is bonded to four atoms of different type. The c-BN lattice can be envisioned as stacked six-membered rings, with each ring in the chair conformation. BN also has disordered forms: (1) amorphous form (a-BN) with a full atomic disorder, (2) partially disordered turbostratic form (t-BN), containing randomly distributed h-BN rings, and (3) disordered tetrahedral amorphous form with dominantly sp^3 structures, which we call ta-BN by analogy to a similar structure of carbon.[2]

Similar to diamond, c-BN has outstanding physical and chemical properties, like are high thermal conductivity, superhardness, transparency. In addition, c-BN has higher thermal and chemical stability than diamond in a wide temperature range, making c-BN a good alternative under the extreme conditions. A principal difference between boron nitride and carbon structures is that a BN structure has a mixed ionic and covalent bond, while bonding in a carbon structure is strictly covalent. This causes differences in thermal and electrical conductivities as well as in a finite band gap. h-BN has a bandgap of 5.2 eV.[3] The Knoop-hardness of diamond is 100 GPa, while that of c-BN is 45 GPa.[4] Higher oxidation resistance than diamond gives c-BN advantage in machining. The diamond films can be doped only with p dopants, while c-BN can be doped with both n and p dopants and even combined with insulating boron-oxide layer.

Since the first synthesis of c-BN by Wentorf in 1957,[5] performed under high pressure (>6.2 GPa) and high temperature (>1620 K), the starting point for most studies has been the generally accepted equilibrium phase (P,T) diagram of h-BN-c-BN (Figure 1) proposed by Corrigan and Bundy.[6] According to that diagram, the h-BN−c-BN−liquid triple point occurs at 3500 K and 9.5 GPa, and only the metastable c-BN phase is present for ambient pressure at all temperatures. Pure-phase c-BN can be synthesized near the triple point at high temperatures and pressures, which, in practice, are expensive to reach. However, not only is compression needed for the phase transformation, but also

Received: November 6, 2017
Revised: December 5, 2017
Published: December 6, 2017

DOI: 10.1021/acs.jpcc.7b10955
J. Phys. Chem. C XXXX, XXX, XXX−XXX

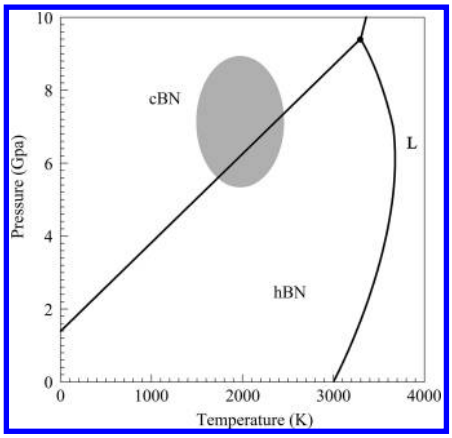

Figure 1. BN phase diagram showing $P-T$ phase space of stability of h-BN, c-BN, and L (liquid BN) due to Bundy.[6] Shaded area represents the approximate phase space considered in our simulations.

the sp^2-ordered network has to be broken and sp^3 network has to be reconstructed. Thus, while high temperature overcomes the energy barrier for the process, the pressure modifies the electronic arrangement.

Decrease in the pressure and temperature in the *c*-BN synthesis has been the main target for long time. One way to reduce pressure and temperature to a certain extent has been use of various multicomponent catalysts in so-called indirect methods. The catalytic method is currently the main method for obtaining industrial c-BN.[7−11] The use of poorly ordered t-BN and a-BN as the starting materials instead of well-crystallized highly ordered h-BN has also been extensively investigated.[11]

Thermodynamically, the phase transformation is accompanied by the decrease in the Gibb's free energy. While c-BN and h-BN phases can exist together, one phase has a minimal free energy, while the other one could be thermodynamically metastable. When a cluster gets smaller, the surface effects become dominant over the bulk effects. The surface of nanoparticles exposes a number of dangling bonds. If these are not passivated by hydrogen, then surface reconstruction may take place. According to Young−Laplace equation,[12−14] the surface tension induces internal pressure in the (spherical, quasi-isotropic) nanoparticle, $P_i = 2\gamma/r$, where γ is surface energy (which is for graphite about $\gamma_G \approx 3.1$ J/m^2, for diamond $\gamma_D \approx 3.7$ J/m^2,[15] and in the same range of values for h-BN and c-BN). Obviously P_i decreases from diamond to graphite, and the diamond surface would have tendency to graphitize, leading to a so called "bucky-diamond". Interestingly, in the case of a c-BN nanoparticle with radius of 1 nm, assuming $\gamma \approx 3$J/m^2 gives internal pressure of ∼7 GPa, sufficient to bring c-BN into the stable phase, Figure 1. The shaded area covers conditions of size and internal pressure for the cases used in the present paper, showing the existence of a stable c-BN core within the bucky-cBNs, obtained in our calculations.

The synthesis of diamond from graphite, by both direct and indirect methods, is studied much more than the synthesis of c-BN, so the comparison of c-BN and diamond synthesis might be beneficial. The transformation of nanodiamond clusters into sp^2 forms such as fullerenes, onion-like-carbon, and the mixed structures collectively termed bucky-diamonds (diamond-like core encased in an onion-like shell) has been successfully simulated and experimentally observed.[16,17] Most of the theories predict nanodiamond to be the stable phase of carbon in the range less than about 5 to 6 nm.[18,19]

The diamond nucleation could be enhanced at ambient pressures, when the transformation into graphite phase is inhibited, for example, by the atomic hydrogen. Hydrogen plays an important role in nanodiamond synthesis at ambient pressures, as demonstrated by a number of experiments,[19−22] where hydrogen induced sp^3 hybridization of carbon atoms, increasing both the stability of nanodiamonds and the rate of their production.[23,24] The actual crossover of particle stability between graphite and diamond phase depends on the nanoparticle size, hydrogen concentration, and temperature.

We report a computational study on the effects of hydrogen to the mutual transformability of h-BN to c-BN (and vice versa) at ambient pressure, in a range of temperature of 1500−2500 K, using quantum-classical molecular dynamics (QCMD). We identify details of a number of processes leading to nanosized c-BN, similar to those observed in the graphite-to-diamond transformation in the presence of hydrogen.

COMPUTATIONAL DETAILS

We use quantum-classical molecular dynamics (QCMD), where the quantum electronic structure calculations are performed using the density functional tight-binding (DFTB) method,[25] while the heavy particle motions are calculated by classical dynamics. This method has been shown to be highly applicable to the boron nitride nanostructures.[26−28] The method uses predefined Slater-Koster pair potentials and is, by using only valence electrons and integral parametrization, simpler and faster than the first-principles DFT methods. Although it is two to three orders of magnitude slower than classical molecular dynamics, it is firmly based on quantum mechanics and can be applied to large systems where it gains two to three orders of magnitude computing acceleration in comparison with the DFT methods. For all calculations, we employ the matsci-03 parameter set,[29] as it contains pair potentials for all chemical elements in our present study, and the combination of DFTB and this parameter set was previously extensively tested against first-principles DFT.[27]

In the QCMD simulations, we use the velocity verlet algorithm with a time step of 1 fs, small enough to keep kinetic energy of not being lost due to discretization of time.[27,28] We further use the Nosé−Hoover chain thermostat[30] with three links to keep the nanosystem at a constant temperature T. It provides a way to simulate a system which is (asymptotically, i.e., at large time) in the NVT canonical ensemble. The kinetic energy oscillates around approximately $\frac{3}{2}nkT$, as required by equipartition of the number of atoms in the model system, n. The system includes nanocluster and, possibly, impacting particles of mass M, which has initial velocity of its center of mass calculated as $v_i = \sqrt{\frac{3kT}{M_i}}$. As in our previous work, the geometry of irradiation is isotropic, with a single nitrogen atom emitted each 4 ps randomly from a sphere of radius 3 nm toward the instantaneous center of mass of the target BN nanostructure.[28] The same methodology of irradiation is used when H or NH are projectiles, except for the adaptation to the adequate mass and temperature. Particles (atoms and molecules) ejected out from the cluster are removed from the system before the next impacting particle is emitted, when they reach the 3 nm spherical border. These choices are implemented by self-made interface code[31] to simulate the

DOI: 10.1021/acs.jpcc.7b10955
J. Phys. Chem. C XXXX, XXX, XXX−XXX

actual plasma conditions of high-pressure electrical arc, which needs to be regarded as an open system for the purpose of our simulations. These conditions regulate the flux and temperature of impacting particles. Thus one particle in the 3 nm spherical vicinity of the target cluster results in plasma concentration of $\sim 8.8 \times 10^{18}$ cm^{-3}, which corresponds to pressure of ~2.4 atm at 2000 K, not much different from the pressure of the plasma in a typical high pressure electric arc. The temperature of the arc in the plasma column reaches 10 000 K, but in the external regions it gradually decreases toward room temperature. Finally, the ionization degree of the arc plasma is low, ~1%, which justifies consideration of electrically neutral impacting particles.

The typical spatial range of the Slater-Koster electronic potentials is ~5 Å, with even shorter repulsive potentials. To speed up the calculation, we do not use long-range dispersions, self-consistent charge, or magnetic polarization corrections. The latter have been shown to have minimal effect to the calculation outcome for boron nitride systems.[32]

It is known that H preferentially adsorbs on boron atoms at low coverage, while adsorption on nitrogen atoms is metastable.[33] It has been found that treatment of the surface of sp^2-hybridized boron nitride by excited hydrogen atoms leads to termination of the π dangling bonds and transformation to the sp^3 boron nitride.[34] We verified that DFTB correctly predicts stronger bonding of H atoms to B than N by performing corresponding DFT benchmark calculations (Supporting Information S1). In both cases, the ground-state H chemisorption on h-BN changes the hybridization of B from sp^2 to sp^3, accompanied by a pyramidalization of the initial planar surface. In the presence of atomic H, sp^3 hybridization is dominating, while without H, sp^2 is more preferable.

RESULTS AND DISCUSSION

We have considered three cases that led to buildup of a c-BN crystal, fully or partially enclosed in a h-BN cage, which we call bucky-cBN, by analogy to the bucky-diamond. In the first case, the amorphous cluster B_{144} is irradiated with nitrogen atoms and with NH molecules. The former one leads to an onion-like double-wall (DW) BN cage, and in the latter a bucky-cBN is produced. In the second case, a DWBN cage, obtained by exposure of a boron amorphous cluster B_{96} to N atoms, is irradiated by H atoms, producing c-BN. These two processes take place at 2000 K. The third case presents the phase transformation of a ta-BN nanoparticle, obtained by irradiation of a B_{144} cluster by NH molecules at 1500 K, to c-BN by heating to 2000 K. By further heating to 2500 K this c-BN transforms to a single-wall h-BN cage. The minimum size of an initial boron cluster, B_{96}, is essential for obtaining a bucky-cBN growth in either of these cases. Important factor in these transformations is temperature, considered here in range 1500−2500 K. A smaller size than B_{96} would lead, under the conditions of this work, to various interesting BN structures but not to a c-BN. Thus B_{36} and B_{72} lead to a single-wall cage when exposed to N atoms and a BN flake when irradiated with NH molecules, except at 1500 K when B_{72} produces ta-BN structures. For the cases reported here, B_{96} and B_{144} could not build c-BN or bucky-cBN at 2500 K when irradiated with NH molecules, while simulations at 1500 K led to ta-BN structures. The simulations at 2000 K with initial B_{192} irradiated by N and NH yield the structures similar to the B_{144} cases, indicating that similar BN structures can be obtained with even bigger initial boron clusters with sufficient N and H feed. Because of computation limitations, we could deal only with ultrananosize structures, smaller than 2 nm.

Choice of a boron cluster as a target in the considered cases is inspired by recent experiments. Kim et al.[35] has reported high-yield BNNT production upon dissociation of the boron nitride (h-BN) powder feed in the high-temperature plasma (>8000 K) at atmospheric pressure. The boron atoms then associated in the boron clusters while moving to colder plasma regions and reacted with nitrogen, hydrogen, and their compounds building the BN nanostructures. Zettl et al.[36] used plasma torch in nitrogen atmosphere at high pressure with boron feedstock, the latter evolving into boron droplets and interacting with N.

Changing BN Phases by Particle Irradiation. We first consider the amorphous boron cluster of 144 atoms (B_{144}) at T = 2000 K, irradiated by 500 nitrogen atoms (N) with thermal velocity corresponding to T, as defined in computational methods. Irradiation of the B_{144} cluster by N and NH at 2000 K, leads to onion-like, double-wall h-BN cage and to bucky-BN, respectively (Figure 2a, Movies 1 and 2). Each set of these

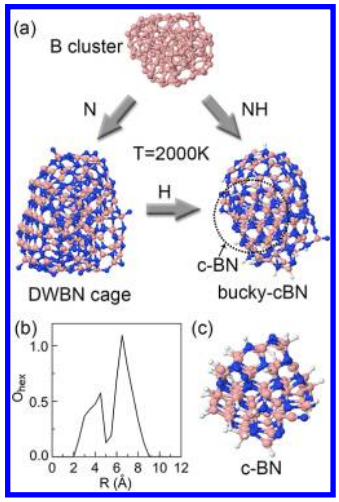

Figure 2. (a) Irradiations of B cluster with nitrogen atoms (left) and NH molecules (right) at 2000 K produce double-wall BN nanocage (DWBN) and bucky-cBN, respectively. Irradiation of DWBN by H leads to a bucky-cBN or hydrogenated c-BN, shown in panel c. The c-BN core in a bucky-cBN is encircled. (b) Radial hexagon density distribution as a function of distance from the nanocluster center of mass (explained in the text).

results comes from three of four independent simulations. Only one case with either N or NH irradiation led to a single-wall h-BN cage. A similar outcome was obtained with irradiation of B_{96} by N and NH at 2000 K. To establish distinguishability of external and internal shells of the DWBN cage structure, we sliced the space by many concentric layers from the center of mass of the nanostructure and obtained a radial distribution function for the purely alternating B−N hexagons. The counting of hexagonal rings and atoms was performed at each 0.5 Å in radial direction, with a thickness of 1 Å for each layered bin (±0.5 Å from the represented distance). The number of hexagonal rings in each concentric layered bin is calculated by ring counting code.[37] A thickness of 1 Å was chosen because only atoms within each layered bin were used for ring counting, and a ring is not complete if any atom in the ring is excluded by binning. Absolute counts of atoms or hexagonal rings were divided by the volume of each layered bin,

DOI: 10.1021/acs.jpcc.7b10955
J. Phys. Chem. C XXXX, XXX, XXX−XXX

and we got the radial hexagon density distribution that shows how dense the atoms are distributed at different distances. The "noise" is reduced by taking the average of counts over the last 1 ps of each N impact. The result is shown in Figure 2b, clearly indicating the creation of double-wall layers in an "onion"-like structure. The irradiation of DWBN cage by hydrogen atoms at 2000 K leads to a c-BN structure (Figure 2c and Movie 3), the properties of which will be discussed later.

As explained in the Computational Details section, atoms (N or H) or molecules (NH) are added each 4 ps to the system. Upon reaching the cluster surface, the particles could be either bonded or reflected. Simultaneously, atoms or molecules might be emitted from the cluster and removed from the system when they reach the 3 nm surface. In Figure 3, left panel, we show the

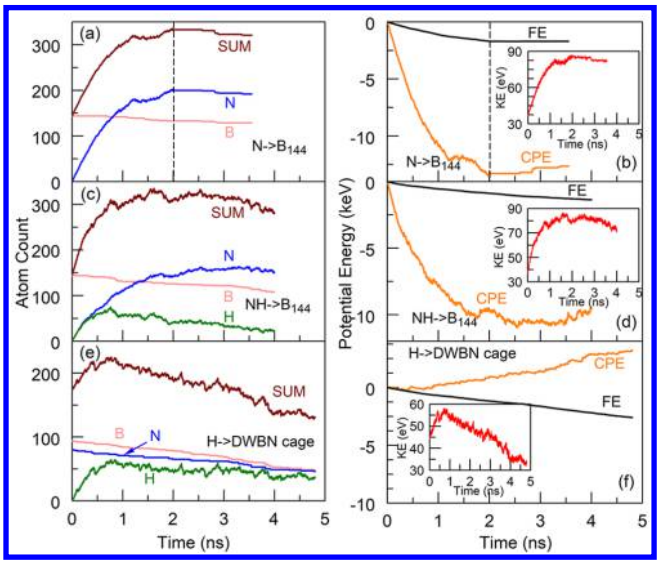

Figure 3. Atoms count and energy balance of cluster in a progression of impacts in 4 ps intervals. (a,b) Cluster B_{144} irradiated by N. (c,d) Cluster B_{144} irradiated by NH. (e,f) DWBN, obtained from B_{96} irradiated by N, exposed to irradiation of H. In all cases the temperature is kept at 2000 K. CPE, KE, and FE in panels b, d, and f represent potential energy, kinetic energy, and change of the formation enthalpy of each cluster, respectively.

number of atomic particles in each of the three irradiated system as a function of time. As can be seen in Figure 3a, the number of boron atoms slightly decreases by ejection from the initial boron cluster. However, the number of implanted nitrogen atoms increases, with an efficiency close to 50%. Because the created BN structure can be unstable under unnecessary further impact of N atoms, which might create attached nitrogen chains, the irradiation could stop once the number of N atoms is similar, somewhat bigger than number of B atoms (vertical dashed line in Figure 3a). We let the system in Figure 3a evolve for a prolonged time without irradiation by N atoms to confirm its stability. The N count is saturating when the numbers of B and N atoms are approximately equal because N is not easily "finding" a place to bond but is rather reflected or bonded in short N chains, which are unstable and typically emit N_2 molecules.

As discussed in the Computational Details section, we use the Nosé–Hoover chain thermostat exchanging energy with an "infinite" reservoir, and thus our system is locally in NVT canonical ensemble. However, the number n of particles in our system is not conserved because, on one hand, we add particles by irradiating the system and, on the other hand, the system occasionally emits particles. Although the target temperature T is kept constant, the kinetic energy of the system is calculated as $\frac{3}{2}nkT$ and is not constant because n is changing. All of these processes move the system to a strong nonequilibrium regime. In Figure 3, right panel, we combine the cluster potential (CPE) and kinetic (KE) energies, as obtained from the quantum electronic DFTB calculation with the change of formation enthalpy (FE) between instantaneous cluster (at time t) and the initial cluster (at $t = 0$) for each of the considered system, showing them as functions of time. The details of our calculations of the change of formation enthalpy are explained in Supporting Information S2. The potential energy of the growing cluster is increasing in absolute value in Figure 3b) and so is the kinetic energy (inset at Figure 3b) because the total number of atoms bonded to the cluster is increasing while irradiated by N atoms. Similar conclusions can be drawn with NH projectiles (Figure 3c,d), in which case the number of impacting molecules needs to be more than two times larger than in the case of impact N atoms. NH is dissociating at the surface of the target cluster and the number of implanted H atoms saturates much earlier than N atoms. Upon saturation, the number of implanted H atoms reaches ~25% of the total number of B+N atoms and decreases by further NH irradiation. The CPE is first decreasing due to implantation of N and H atoms and then increasing because of the loss (ejection) of atoms from the cluster. Still, the formation enthalpy (FE) is negative and almost linearly decreasing, reflecting the exoergic processes in which stability (i.e., bonding energy) increases, even when the number of atoms in the cluster saturates, or even decreases. This reflects the system tendency to spontaneously reorganize to more stable configurations. In the case of DWBN irradiated by H (Figure 3e,f), the initial contents of B and N in the cluster are approximately equal (the difference reflects the existence of defects), while the number of implanted hydrogen atoms increases until reaching ~90% of the number of B and N, then saturates. When the total number of atoms in the cluster starts decreasing (Figure 3e), the absolute value of potential energy and kinetic energy of the cluster decrease. However, in this case, the formation enthalpy (FE) also decreases approximately linearly with time, reflecting reorganization of the system into bucky-cBN. The thermodynamics of the cluster during the process, that is, the thermal contributions including the entropy of the vibrational, rotational, and translational motion at 2000 K, are considered separately in Supporting Information S3. These contributions are, like kinetic energies in Figure 3b,d,f, about one order of magnitude smaller than change in the formation enthalpy and will not change the trend of the systems toward greater stability at 2000 K.

The Lindemann index is a useful parameter to measure the thermally driven disorder in our clusters. The Lindemann index is calculated as follows[38]

$$\delta = \frac{2}{N(N-1)} \sum_{i<j} \frac{\sqrt{\langle r_{ij}^2 \rangle - \langle r_{ij}^2 \rangle}}{\langle r_{ij} \rangle} \quad (1)$$

where r_{ij} is the distance between ith and jth atoms, N is the number of atoms in the system, and the average was calculated over the last 2 ps in each 4 ps time slot (to exclude the spurious effects that would result during the approach of an incident particles to the cluster).

DOI: 10.1021/acs.jpcc.7b10955
J. Phys. Chem. C XXXX, XXX, XXX−XXX

Typically, the Lindemann index is above 0.1 for liquid phase and is below 0.1 for a more ordered solid phase. In Figure 4 it

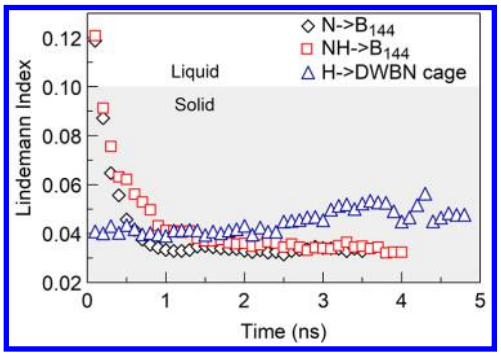

Figure 4. Thermal disorder as measured by Lindemann index in various scenarios of irradiation. The liquid B_{144} droplet is quickly converted to solids (after ~50 N or NH impacts, i.e., after ~200 ps). The solid-phase DWBN somewhat increases disorder in bombardment by H.

follows, for various cases shown in Figure 3, the change of the liquid to solid phase in the process of irradiation. The structures represented by Figure 3a,c start with a liquid boron cluster, which converts to a solid crystal BN structure upon irradiation with N and NH particles. In the case represented by Figure 3e, both initial and final phases are solid, as indicated by the Lindemann index.

To track the quality of the created BN nanostructures following the dynamics of implantation of N and H, we followed the hybridization of each atom in the cluster, determined by the atom coordination number (3 for sp^2, 4 for sp^3) as well as the type of the atoms in the coordination. While h-BN structures contain sp^2-hybridized B and N atoms, c-BN structures are characterized by sp^3 hybridization of the atoms. The ratios of the sums of the sp^3-hybridized B and N atoms and sums of the sp^2-hybridized B and N atoms, where sums are averaged over each 100 ps, are shown in Figure 5 as a

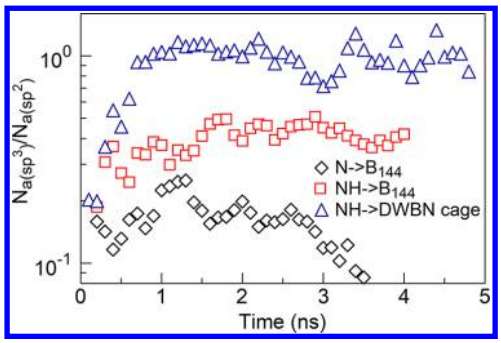

Figure 5. Evolution of the ratios of the sp^3- and sp^2-hybridized atoms (summed over B and N), averaged over 100 ps for various conditions of irradiation.

function of irradiation time. Because there is one system not containing H atoms, to make the parameter comparable between all cases, we counted atoms that are coordinated only with N (in the case of B) or only with B (in the case of N), which we call "pure" hybrids. In the case of N irradiation of B_{144} creating DWBN cage, the sp^2-hybridized atoms dominate, with only up to 0.2 fraction of sp^3-hybridized atoms, which came from the cross bonding of the inner and outer "onion" shells. In the other two cases where c-BN clusters are created, the proportions of sp^3-hybridized atoms are higher. Bucky-cBN has a ratio between DWBN cage and c-BN because this structure is a combination of sp^2 structure (cage) and sp^3 structure (c-BN).

Another check of short-range order in the created structure is the ring count. We count all BN rings numbered from 3 to 7 and present them in Figure 6. The hexagons are strongly

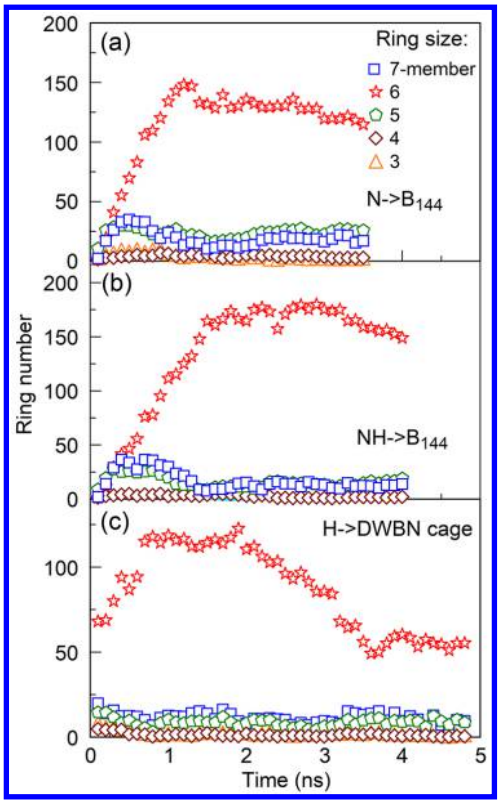

Figure 6. Number of rings of various sizes formed by irradiation of a boron cluster B_{144} with (a) N and (b) NH and by (c) irradiation of DWBN cage by H.

dominant in the mature phases of all considered nanostructure evolution, while the rings of other sizes in most cases are associated with the defects in the created BN lattice. It is interesting that in all three cases, heptagons and pentagons are dominant defects, with slight advantage of heptagons. The situation is reminiscent of the appearance of haeckelite penta-heptatite defects in graphene formation.[39] These defects are dominant rings for the first hundred of impacts, as shown in Figure 6a,b.

Domination of the hexagon structures is not a sufficient criterium for establishing the crystallineity of a BN structure. It may happen that some of the hexagon rings are all made of nitrogen or boron, or simply have a defect nonalternating B−N structure. In a perfect structure composed of the sp^2 type BN atoms, each atom is connected to 3 hexagonal rings. In counting the total number of rings, each ring is counted six times. Thus, with total number K of both N and B sp^2, number of perfect hexagonal rings is estimated to be $hex_{sp^2} = 3K/6 = 0.5$ K. In a perfect structure composed of sp^3-type hybridized atoms, each atom has four bonds (Supporting Information S4). If we choose any two of these four bonds, we find that they lead to two different hexagonal rings (not necessarily coplanar). Number of choices is six and so each atom is associated with

DOI: 10.1021/acs.jpcc.7b10955
J. Phys. Chem. C XXXX, XXX, XXX−XXX

6*2 = 12 hexagonal rings. Therefore, with total number of sp^3 N and B atoms equals M, number of estimated perfect hexagonal rings is $hex_{sp}^3 = 12M/6 = 2$ M. This analysis is shown in Figure 7 for the cases of irradiation leading to bucky-cBN.

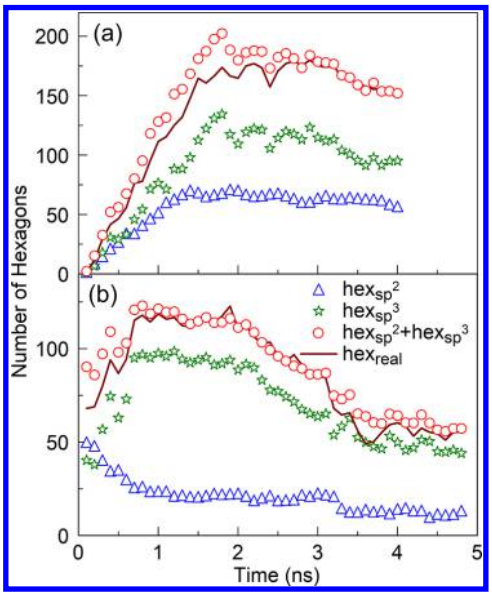

Figure 7. Analysis of the hexagon types: (a) Boron cluster B_{144} irradiated by NH at 2000 K. (b) Double-wall BN cage irradiated by H at 2000 K.

Although the total number of hexagons is close to the ideal number (estimate curve, hex_{sp2} + hex_{sp3}, in Figure 7a), the "ideal" hexagons carrying "pure" sp^3 atoms and thus representing the c-BN built are dominating, by a factor of ~2 to the sp^2 hexagons. Similarly, hex_{sp3} are dominating by far over hex_{sp2} in Figure 7b, showing the dominant process in this case—transformation to the c-BN, with much less h-BN enclosing or attached. This indicates that "onion-like" h-BNs can serve as precursors for quality c-BN synthesis in a H plasma at ambient pressure.

The total number of hexagons starts to decrease after 2 ns, as shown in Figure 7, reflecting the ejection of boron atoms from cluster while boron atoms are not supplied from irradiation (Figure 3c,e). This raises the question of thermodynamic stability of the created c-BNs and bucky-cBNs. Therefore, the created c-BNs and bucky-cBNs are kept at 2000 K without irradiation for 1 ns. Only a few N and H atoms left in form of N_2 and H_2 at the beginning of this process, and the original structures stay stable for 1 ns. Slowly cooling all structures to 500 K does not change their structure.

Changing BN Phases by Heating. So far we have discussed the transformation of a boron cluster at 2000 K to bucky-cBN under the irradiation of NH molecules. If the NH irradiation is applied to B_{144} cluster at 1500 K, then an amorphous structure is formed (Figure 8a and Movie 4), which is a mixture of disordered sp^2 structures (similar to turbostratic BN, t-BN) and disordered sp^3 structures (ta-BN) in the core. The analysis of creation and configuration of this disordered structure is shown in the Supporting Information S5. However, when this structure is exposed to heating, at temperature of 2000 K for prolonged time (~1.5 ns), a bucky-cBN structure is formed, with a c-BN core enclosed by irregular h-BN cage, as shown in Figure 8b and Movie 5. In this process, the sp^3

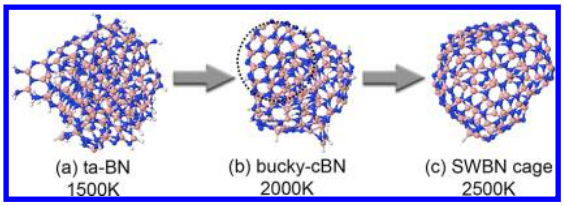

Figure 8. Process of transformation into bucky-cBN when heating t-BN from 1500 to 2000 K. Heating of the bucky-cBN from 2000 to 2500 K yields a single-wall h-BN cage.

irregular core transforms into a c-BN core, while t-BN part transforms into an h-BN ordered structure. It is interesting to note that a similar process has been discussed with respect to transformation by heating of a disordered sp^3 carbon structures into diamond cores.[40] If a bucky-cBN is heated from 2000 to 2500 K, it transforms to a single-wall h-BN structure (Figure 8c and Movie 6), similar to a process that exists in carbon nanodiamond.[41] In both processes, heating of the amorphous structure to 2000 K (Figure 9b) and bucky-cBN to 2500 K (Figure 9a) causes hydrogen to be emitted in significant quantities, especially in the latter case in which also boron and nitrogen are emitted until reaching the equal numbers B and N atoms, as necessary for a defectless h-BN cage.

We found that possibly the best insight into the transformation of the disordered sp^3 structure can be obtained from an analysis of the bond angles of the initial amorphous BN structure and the final c-BN structure. The angle is measured as between bond "1−2" composed of N and B atoms (referring to the atomic number labels in Figure 10a) and the three N−B bonds originating from N atoms labeled with "3". Thus in a perfect c-BN structure (shown in Figure 10a) one of these three angles should be 0°, while the other two angles are 109.47°. In a disordered ta-BN structure, like the one obtained at T = 1500 K (representative case t = 0 shown in Figure 10a), the disorder is reflected by the width of the distribution of various angles, peaked at ~12° and ~115°. As the cluster remains at 2000 K, the width of angular distributions decreases, and peaks, respectively, shift toward 0 and 110°, showing the ordering toward a c-BN core. We ended the simulation of this evolution at 1.47 ns.

A controlled test shows hydrogen's critical role in creating and preserving the number of sp^3-hybridized atoms in BN structures. We modified the initial amorphous structure by removing all hydrogen atoms and preserving the original geometry of boron and nitrogen atoms. This hydrogen-free cluster was then subjected to the same heating process to 2000 K. As opposed to the transformation from ta-BN to c-BN that has been shown before, transformation process of the hydrogen free ta-BN structure shows the formation of a double-wall cage structure instead of the bucky-cBN structure. The comparison of the ratios of sp^3- to sp^2-hybridized atoms in the two cases clearly shows a larger ratio in the hydrogen-containing cluster than the hydrogen-free cluster, as illustrated in Figure 11. For the transformation from bucky-cBN to single-wall BN cage at 2500 K, this ratio keeps reducing, eventually reaching zero. This is consistent with the change of number of H atoms in cluster, as observed in Figure 9c.

The bucky-cBN subject to a sudden change of temperature from 2000 to 2500 K shows conversion of the phase via a partially disordered bucky system to a highly ordered h-BN cage (Figure 12a), reflected by a steep change of the Lindemann index in range 550−650 ps. The steep drop of

DOI: 10.1021/acs.jpcc.7b10955
J. Phys. Chem. C XXXX, XXX, XXX−XXX

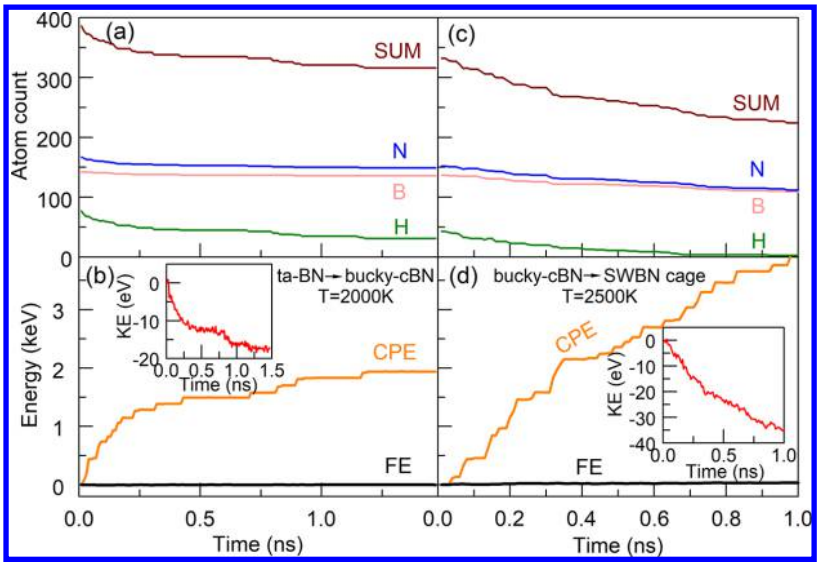

Figure 9. Number of atoms in cluster and energy balance as a function of time for (a,b) bucky c-BN at 2000 K and (c,d) h-BN cage at 2500 K. CPE, KE, and FE in panels b and d represent potential energy, kinetic energy, and change of formation enthalpy of each cluster, respectively.

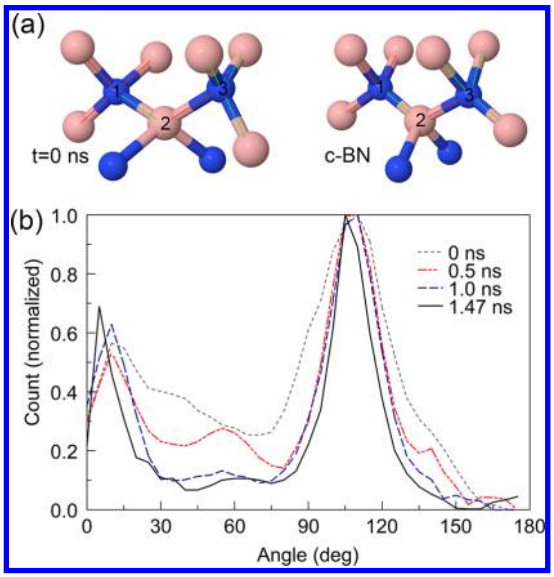

Figure 10. (a) Angles between N1−B2 and N3−B's for a disordered sp^3 bonds (upper) and ideal c-BN sp^3 structure. (b) Distributions of angles shown in panel a for various times as system changes from disordered c-BN structure to a bucky-cBN. The angles are calculated only when there are three sp^3 atoms bonding in a chain form.

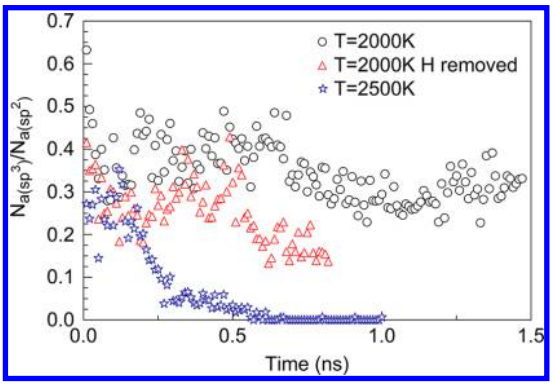

Figure 11. Evolution of the ratios of the sp^3- and sp^2-hybridized atoms (summed over B and N) for transformations (1) from t-BN cluster at 1500 K to bucky-cBN at 2000 K, (2) from amorphous cluster with only hydrogen atoms removed to double-wall cage at 2000 K, and (3) from bucky-cBN at 2000 K to single-wall cage at 2500 K. Each data point is an average value in 100 ps time interval.

the sp^3-type hexagons in the BN structure at 2500 K is also visible at Figure 12b, showing complete conversion of the hexagons to sp^2 type (hex_{sp2}). The defects of the final cage structure are present mainly in the form of pentagons, which reach ~25% of all polygons.

CONCLUSIONS

We have shown, using high-temperature quantum-classical molecular dynamics, that atomic hydrogen could play a decisive role in synthesis of cubic boron nitride at high temperatures (1500−2500 K) and normal pressures. The atomic hydrogen is catalyzing the sp^3 hybridization of B and N atoms, restraining growth of the h-BN phase and resulting in a c-BN core partially or completely encapsulated by a h-BN cage-like structure. We consider transformation from a liquid boron cluster at 2000 K to bucky-cBN when irradiated by NH molecules as well as transformation of a DWBN cage to c-BN when irradiated by H atoms. Heating a tetrahedral amorphous boron nitride (t-BN with a ta-BN core) cluster results in bucky-cBN, too. Further heating of the bucky-cBN eliminates the c-BN core and transforms the structure into a SWBN cage. The created structures are stable both at the respective temperatures and by gradual cooling to temperatures as low as 500 K. By checking the change of the ratio of sp^3 to sp^2 atoms as well as corresponding BN rings, we closely follow the evolution of the c-BN and h-BN content and their quality. We have developed and applied procedure for calculation of the formation enthalpies during the process of formation of the bucky-cBN structures. The free energies show that these exoergic transformations, through the changes of the atom content and number, evolve gradually toward the structures of increasing stability. We expect that our findings and analysis, reminiscent to the similar hydrogen role in nanodiamond production, will inspire further theoretical and experimental research on hydrogen effects in the synthesis of the boron

DOI: 10.1021/acs.jpcc.7b10955
J. Phys. Chem. C XXXX, XXX, XXX−XXX

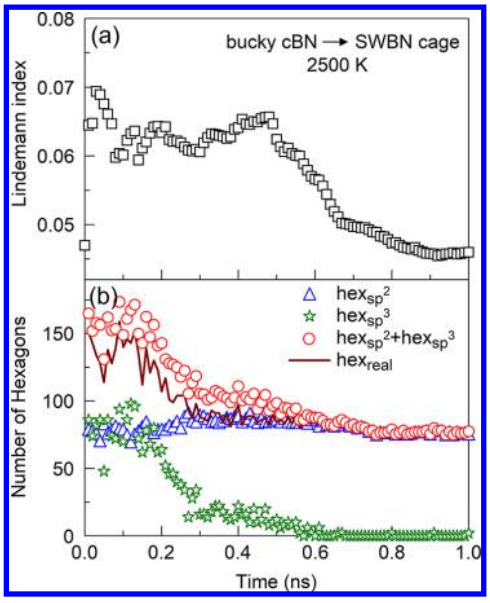

Figure 12. (a) Evolution of the Lindemann index during heating of the bucky-cBN to 2500 K. Phase change to h-BN cage is visible by steep change of the Index at time ~500 ps. (b) Conversion of the hexagon types in time.

nitride nanostructures at high temperatures and ambient pressures, like those present in the arc plasma.

■ ASSOCIATED CONTENT

Supporting Information

The Supporting Information is available free of charge on the ACS Publications website at DOI: 10.1021/acs.jpcc.7b10955.

S1. Hydrogen effect on the hybridization of B and N atoms. S2. Calculation of the formation enthalpy. S3. Thermal entropy change. S4. Structure of ideal c-BN. S5. Analysis of the ta-BN structure at 1500 K. (PDF)

B_{144} cluster under irradiation of N atoms at 2000 K, creating double-wall BN (DWBN) cage in 2 ns. (AVI)

B_{144} cluster under irradiation of NH molecules at 2000 K, creating bucky-cBN in 4 ns. (AVI)

DWBN cage under irradiation of H atoms at 2000 K, creating c-BN nanocrystal in 4.8 ns. (AVI)

B_{144} cluster under irradiation of NH molecules at 1500 K, creating ta-BN in 3.2 ns. (AVI)

Transformation of ta-BN to bucky-cBN by heating cluster to 2000 K, in 1.47 ns. (AVI)

Transformation of bucky-cBN to single-wall BN cage by heating cluster to 2500 K, in 1 ns. (AVI)

■ AUTHOR INFORMATION

Corresponding Author

*E-mail: predrag.krstic@stonybrook.edu.

ORCID

Predrag Krstic: 0000-0001-8326-2978

Notes

The authors declare no competing financial interest.

■ ACKNOWLEDGMENTS

This work was supported by the U.S. Department of Energy, Office of Science, Basic Energy Sciences, Material Sciences and Engineering Division Grant No. DE-AC02-09CH11466. Presented results were in part calculated using XSEDE computing facilities (UCSD's Comet) and computing facilities (LIred and SeaWulf) of IACS at SBU. We acknowledge the whole Nanosynthesis team of the Princeton Plasma Physics Laboratory for constructive discussions. We are grateful to Stephan Irle of ORNL for inspiring and thorough discussions on the nanosynthesis and thermochemistry.

■ REFERENCES

(1) *Properties of Advanced Semiconductor Materials: GaN, AlN, InN, BN, SiC, SiGe*; Levinshtein, M. E., Rumyantsev, S. L., Shur, M. S., Eds.; John Wiley & Sons: New York, 2001.

(2) Marks, N. A. Thin film deposition of tetrahedral amorphous carbon: a molecular dynamics study. *Diamond Relat. Mater.* **2005**, *14*, 1223−1231.

(3) Paine, R. T.; Narula, C. K. Synthetic routes to boron nitride. *Chem. Rev.* **1990**, *90*, 73−91.

(4) Schwetz, K. A. Boron Carbide, Boron Nitride, And Metal Borides. *Ullmann's Encyclopedia of Industrial Chemistry*; Wiley-VCH: Weinheim, Germany, 2000.

(5) Wentorf, R. H., Jr Cubic form of boron nitride. *J. Chem. Phys.* **1957**, *26*, 956−956.

(6) Corrigan, F. R.; Bundy, F. P. Direct transitions among the allotropic forms of boron nitride at high pressures and temperatures. *J. Chem. Phys.* **1975**, *63*, 3812−3820.

(7) Bocquillon, G.; Loriers-Susse, C.; Loriers, J. Synthesis of cubic boron nitride using Mg and pure or M′-doped Li_3N, Ca_3N_2 and Mg_3N_2 with M′= Al, B, Si, Ti. *J. Mater. Sci.* **1993**, *28*, 3547−3556.

(8) Lorenz, H.; Orgzall, I. Formation of cubic boron nitride in the system Mg_3N_2-BN: a new contribution to the phase diagram. *Diamond Relat. Mater.* **1995**, *4*, 1046−1049.

(9) Lorenz, H.; Orgzall, I.; Hinze, E. Rapid formation of cubic boron nitride in the system Mg_3N_2-BN. *Diamond Relat. Mater.* **1995**, *4*, 1050−1055.

(10) Vel, L.; Demazeau, G.; Etourneau, J. Cubic boron nitride: synthesis, physicochemical properties and applications. *Mater. Sci. Eng., B* **1991**, *10*, 149−164.

(11) Singhal, S. K.; Park, J. K. Synthesis of cubic boron nitride from amorphous boron nitride containing oxide impurity using Mg−Al alloy catalyst solvent. *J. Cryst. Growth* **2004**, *260*, 217−222.

(12) Young, T. *Philos. Trans. R. Soc. London* **1805**, *95*, 65.

(13) Laplace, P. S. *Traite de Mechanique Celeste, Vol. 4, Supplements au Livre X*; Gauthier-Villars: Paris, 1805.

(14) Chen, T.; Chiu, M. S.; Weng, C. N. Derivation of the generalized Young-Laplace equation of curved interfaces in nanoscaled solids. *J. Appl. Phys.* **2006**, *100*, 074308.

(15) Fedosayev, D. V.; Deryagin, B. V.; Varasavskaja, I. G. The crystallization of diamond. *Surf. Coat. Technol.* **1989**, *38*, 1−122.

(16) Barnard, A. S.; Russo, S. P.; Snook, I. K. Modeling of stability and phase transformations in quasi-zero dimensional nanocarbon systems. *J. Comput. Theor. Nanosci.* **2005**, *2*, 180−201.

(17) Kuznetsov, V. L.; Butenko, Yu. V. Nanodiamond graphitization and properties of onion-like carbon. *NATO Science Series, II: Mathematics, Physics and Chemistry (Synthesis, Properties and Applications of Ultrananocrystalline Diamond)* **2005**, *192*, 199−216.

(18) Barnard, A. S.; Russo, S. P.; Snook, I. K. Size dependent phase stability of carbon nanoparticles: Nanodiamond versus fullerenes. *J. Chem. Phys.* **2003**, *118*, 5094−5097.

(19) Spitsyn, B. V.; Bouilov, L. L.; Derjaguin, B. V. Vapor growth of diamond on diamond and other surfaces. *J. Cryst. Growth* **1981**, *52*, 219−226.

(20) Muranaka, Y.; Yamashita, H.; Sato, K.; Miyadera, H. The role of hydrogen in diamond synthesis using a microwave plasma in a CO/H_2 system. *J. Appl. Phys.* **1990**, *67*, 6247−6254.

(21) Angus, J. C.; Hayman, C. C. Low-pressure, metastable growth of diamond and "diamondlike" phases. *Science* **1988**, *241*, 913−921.

DOI: 10.1021/acs.jpcc.7b10955
J. Phys. Chem. C XXXX, XXX, XXX−XXX

(22) Yoshitake, T.; Nishiyama, T.; Nagayama, K. The role of hydrogen and oxygen gas in the growth of carbon thin films by pulsed laser deposition. *Diamond Relat. Mater.* **2000**, *9*, 689−692.
(23) Dementjev, A. P.; Petukhov, M. N. The roles of H and O atoms in diamond growth. *Diamond Relat. Mater.* **1997**, *6*, 486−489.
(24) Mikami, T.; Nakazawa, H.; Kudo, M.; Mashita, M. Effects of hydrogen on film properties of diamond-like carbon films prepared by reactive radio-frequency magnetron sputtering using hydrogen gas. *Thin Solid Films* **2005**, *488*, 87−92.
(25) Aradi, B.; Hourahine, B.; Frauenheim, Th DFTB+, a sparse matrix-based implementation of the DFTB method. *J. Phys. Chem. A* **2007**, *111*, 5678−5684.
(26) Enyashin, A. N.; Ivanovskii, A. L. Graphene-like BN allotropes: Structural and electronic properties from DFTB calculations. *Chem. Phys. Lett.* **2011**, *509*, 143−147.
(27) Ohta, Y. Possible mechanism of BN fullerene formation from a boron cluster: Density-functional tight-binding molecular dynamics simulations. *J. Comput. Chem.* **2016**, *37*, 886−895.
(28) Han, L.; Krstić, P. A path for synthesis of boron-nitride nanostructures in volume of arc plasma. *Nanotechnology* **2017**, *28*, 07LT01.
(29) Lukose, B.; Kuc, A.; Frenzel, J.; Heine, T. On the reticular construction concept of covalent organic frameworks. *Beilstein J. Nanotechnol.* **2010**, *1*, 60−70.
(30) Martyna, G. J.; Klein, M. L.; Tuckerman, M. Nosé-Hoover chains: the canonical ensemble via continuous dynamics. *J. Chem. Phys.* **1992**, *97*, 2635−2643.
(31) Longtao Han's Github. https://github.com/olanky/cBN-project (accessed Nov 3, 2017).
(32) Ohta, Y. Temperature-dependent BN cluster formation dynamics from a boron cluster: Density-functional tight-binding molecular dynamics simulations. *Comput. Mater. Sci.* **2017**, *139*, 16−25.
(33) Weck, P. F.; Kim, E.; Lepp, S. H.; Balakrishnan, N.; Sadeghpour, H. R. Dimer-induced stabilization of H adsorbate cluster on BN (0001) surface. *Phys. Chem. Chem. Phys.* **2008**, *10*, 5184−5187.
(34) Konyashin, I.; Khvostov, V.; Babaev, V.; Guseva, M.; Bill, J.; Aldinger, F. The influence of excited hydrogen species on the surface state of sp^2-hybridized boron nitride. *Diamond Relat. Mater.* **1999**, *8*, 2053−2058.
(35) Kim, K. S.; Kingston, C. T.; Hrdina, A.; Jakubinek, M. B.; Guan, J.; Plunkett, M.; Simard, B. Hydrogen-catalyzed, pilot-scale production of small-diameter boron nitride nanotubes and their macroscopic assemblies. *ACS Nano* **2014**, *8*, 6211−6220.
(36) Fathalizadeh, A.; Pham, T.; Mickelson, W.; Zettl, A. Scaled synthesis of boron nitride nanotubes, nanoribbons, and nanococoons using direct feedstock injection into an extended-pressure, inductively-coupled thermal plasma. *Nano Lett.* **2014**, *14*, 4881−4886.
(37) Tinker Molecular Modeling, 2017. https://dasher.wustl.edu/tinker/.
(38) Lindemann, F. A. The calculation of molecular Eigen-frequencies. *Phys. Z.* **1910**, *11*, 609.
(39) Wang, Y.; Page, A. J.; Nishimoto, Y.; Qian, H.-J.; Morokuma, K.; Irle, S. Template effect in the competition between haeckelite and graphene growth on Ni(111): quantum chemical molecular dynamics simulations. *J. Am. Chem. Soc.* **2011**, *133*, 18837−18842.
(40) Singh, J. Nucleation and growth mechanism of diamond during hot-filament chemical vapour deposition. *J. Mater. Sci.* **1994**, *29*, 2761−2766.
(41) Lee, G. D.; Wang, C. Z.; Yu, J.; Yoon, E.; Ho, K. M. Heat-induced transformation of nanodiamond into a tube-shaped fullerene: A molecular dynamics simulation. *Phys. Rev. Lett.* **2003**, *91*, 265701.

DOI: 10.1021/acs.jpcc.7b10955
J. Phys. Chem. C XXXX, XXX, XXX−XXX